High Fidelity Self-Sorting Assembling of *meso*-Cinchomeronimide Appended *meso-meso* Linked Zn(II) Diporphyrins

Taisuke Kamada,[†] Naoki Aratani,[†] Toshiaki Ikeda,[†] Naoki Shibata,[‡]
Yoshiki Higuchi,*,[‡] Atsushi Wakamiya,[§] Shigehiro Yamaguchi,[§] Kil Suk Kim,[||]
Zin Seok Yoon,[||] Dongho Kim,*,[||] and Atsuhiro Osuka*,[†]

*Contribution from the Department of Chemistry, Graduate School of Science, Kyoto University,
and CREST (Core Research for Evolutional Science and Technology) of Japan Science and
Technology Agency, Sakyo-ku, Kyoto 606-8502, Japan, Graduate School of Life Science,
University of Hyogo, 3-2-1 Koto, Kamigori-cho, Ako-gun, Hyogo 678-1297, Japan, and RIKEN
Harima Institute/SPring-8, 1-1-1 Koto, Mikazuki-cho, Sayo-gun, Hyogo 679-5248, Japan,
Department of Chemistry, Graduate School of Science, Nagoya University, Chikusa,
Nagoya 464-8602, Japan, and Center for Ultrafast Optical Characteristics Control and
Department of Chemistry, Yonsei University, Seoul 120-749, Korea*

Received February 15, 2006; E-mail: osuka@kuchem.kyoto-u.ac.jp; dongho@yonsei.ac.kr; hig@sci.u-hyogo.ac.jp

Abstract: In noncoordinating solvents, *meso*-cinchomeronimide appended Zn(II) porphyrin **2** forms a cyclic trimer, while diporphyrins **7** exhibit high-fidelity self-sorting assembling to form discrete cyclic trimer, tetramer, and pentamer with large association constants from **7**$_{in-in}$, **7**$_{in-out}$, and **7**$_{out-out}$, respectively, through almost perfect discrimination of enantiomeric and conformational differences of the *meso*-cinchomeronimide substituents. In the latter self-sorting processes, the dihedral angles dictated by the two pyridyl nitrogen atoms control the size of the aggregates; the trimer from **7**$_{in-in}$, the tetramer from **7**$_{in-out}$, and the pentamer from **7**$_{out-out}$. Cyclic structures of (**2**)$_3$ and (*R*-**7**$_{out-out}$)$_5$ have been determined by single-crystal X-ray diffraction analysis.

Introduction

Self-sorting is high fidelity recognition of self from nonself and is a common and fundamental property in biological systems. Self-sorting assembling process with discrimination of subtle structural differences among similar isomers may lead to largely different tertiary architectures of variable functions. Structural diversity thus attained plays an important role in many biological processes. In recent years, therefore, diverse efforts have been made toward synthetic supramolecular systems that achieve such high fidelity self-sorting assembling.[1−5]

Metalloporphyrins bearing a coordinating sidearm have been used as an effective platform to build various supramolecular structures with aids of multiple coordination interactions of central metal ions with coordinating sidearms.[6,7] However, such metalloporphyrins have been scarcely tested for self-sorting process. Recently, we have explored three-dimensional porphyrin boxes that are formed via rigorous enantiomeric self-sorting assembling of racemic 4-pyridine-appended *meso−meso* linked Zn(II) diporphyrins, in which the structural matching of 90° dihedral angle between the diporphyrin and the 4-pyridyl group plays a key role toward the formation of box-shaped assemblies.[8] In this case, it has been demonstrated that four molecules of *R*-diporphyrin assemble into *R*-box and four molecules of *S*-diporphyrin assemble into *S*-box via homochiral self-sorting process. Mixed assembling would be expected to lead to polymeric chains or ill-defined assemblies but such assemblies

[†] Department of Chemistry, Graduate School of Science, Kyoto University, and CREST (Core Research for Evolutional Science and Technology) of Japan Science and Technology Agency.

[‡] Graduate School of Life Science, University of Hyogo, and RIKEN Harima Institute/SPring-8.

[§] Department of Chemistry, Graduate School of Science, Nagoya University.

[||] Center for Ultrafast Optical Characteristics Control and Department of Chemistry, Yonsei University.

(1) Stryer, L. *Biochemistry*, 4th ed.; W. H. Freeman: New York, 1995.
(2) (a) Lehn, J.-M. *Science* **2002**, *295*, 2400−2403. (b) Hollingsworth, M. D. *Science* **2002**, *295*, 2410−2413. (c) Krämer, R.; Lehn, J.-M.; Marquis-Rigault, A. *Proc. Natl. Acad. Sci. U.S.A.* **1993**, *90*, 5394−5398.
(3) (a) Wu, A.; Chakraborty, A.; Fettinger, J. C.; Flowers II, R A.; Isaacs, L. *Angew. Chem., Int. Ed.* **2002**, *41*, 4028−4031. (b) Wu, A.; Isaacs, L. *J. Am. Chem. Soc.* **2003**, *125*, 4831−4835. (c) Mukhopadhyay, P.; Wu, A.; Isaacs, L. *J. Org. Chem.* **2004**, *69*, 6157−6164.

(4) (a) Cai, M.; Marlow, A. L.; Fettinger, J. C.; Fabris, D.; Haverlock, T. J.; Moyer, B. A.; Davis, J. T. *Angew. Chem. Int. Ed.* **2000**, *39*, 1283−1285. (b) Shi, X.; Fettinger, J. C.; Cai, M.; Davis, J. T. *Angew. Chem., Int. Ed.* **2000**, *39*, 3124−3127. (c) Cai, M.; Shi, X.; Sidorov, V.; Fabris, D.; Lam, Y.; Davis, J. T. *Tetrahedron* **2002**, *58*, 661−671. (d) Shi, X.; Fettinger, J. C.; Davis, J. T. *J. Am. Chem. Soc.* **2001**, *123*, 6738−6739.
(5) (a) Beijer, F. H.; Sijbesma, R. P.; Kooijman, H.; Spek, A. L.; Meijer, E. W. *J. Am. Chem. Soc.* **1998**, *120*, 6761−6769. (b) Jolliffe, K. A.; Timmerman, P.; Reinhoudt, D. N. *Angew. Chem., Int. Ed.* **1999**, *38*, 933−937. (c) Castellano, R. K.; Nuckolls, C.; Rebek, J. Jr. *J. Am. Chem. Soc.* **1999**, *121*, 1, 11156−11163. (d) Shivanyuk, A.; Rebek, J. Jr. *J. Am. Chem. Soc.* **2002**, *124*, 12074−12075. (e) Corbin, P. S.; Lawless, L. J.; Li, Z.; Ma, Y.; Witmer, M. J.; Zimmerman, S. C. *Proc. Natl. Acad. Sci. U.S.A.* **2002**, *99*, 5099−5104. (f) Ma, Y.; Kolotuchin, S. V.; Zimmerman, S. C. *J. Am. Chem. Soc.* **2002**, *124*, 13757−13769.
(6) (a) Imamura, T.; Fukushima, K. *Coord. Chem. Rev.* **2000**, *198*, 133−156. (b) Wojaczynski, J.; Latos-Grazynski, L. *Coord. Chem. Rev.* **2000**, *204*, 113−171. (c) Iengo, E.; Zangrando, E.; Alessio, E. *Eur. J. Inorg. Chem.* **2003**, 2371−2384. (d) Satake, A.; Kobuke, Y. *Tetrahedron* **2005**, *61*, 13−41, and references therein.

Scheme 1
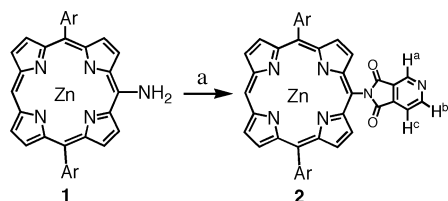
a Cinchomeronic anhydride, pyridine, reflux, 52%. Ar = 3,5-di-*tert*-butylphenyl.

were not observed. Complementary multiple coordination interactions arising from *meso—meso* linked diporphyrin framework help increase the association constants, such that the boxes can be manipulated like covalently linked molecules. One strategy to create assemblies of different shape may be to displace the positions of coordinating nitrogen atoms from the porphyrin plane. This idea drove us to examine self-sorting assembling behaviors of *meso*-cinchomeronimide (3,4-pyridinedicarboximide)-substituted Zn(II) porphyrin **2** and 10,10′-cinchomeronimide-appended *meso—meso* linked Zn(II) diporphyrin **7**. In noncoordinating solvents, the former undergoes complete assembling to form its trimer (**2**)$_3$, whereas the latter is shown to exist as three stable conformers in respect of the orientation of the pyridyl nitrogen atoms, which assemble differently to construct trimeric (**7**)$_3$, tetrameric (**7**)$_4$, and pentameric rings (**7**)$_5$, respectively, through rigorous homochiral self-sorting processes.

Results and Discussion

Synthesis and Characterization. 10-Cinchomeronimide-substituted 5,15-bis(3,5-di-*tert*-butylphenyl) Zn(II)-porphyrin **2** was prepared from condensation reaction of 5-amino-10,20-bis-(3,5-di-*tert*-butylphenyl) Zn(II)-porphyrin[9] **1** with cinchomeronic anhydride in 52% yield (Scheme 1). ^{1}H NMR spectrum of **2** in CDCl$_3$ is very simple, featuring a simple set of peaks with large

(7) (a) Drain, C. M.; Lehn, J.-M. *J. Chem. Soc. Chem. Commun.* **1994**, 2313–2315. (b) Kobuke, Y.; Miyaji, H. *J. Am. Chem. Soc.* **1994**, *116*, 4111–4112. (c) Hunter, C. A. Sarson, L. D. *Angew. Chem., Int. Ed. Engl.* **1994**, *33*, 2313–2316. (d) Wojaczynski, J.; Latos-Grazynski, L. *Inorg. Chem.* **1995**, *34*, 1044–1053. (e) Wojaczynski, J.; Latos-Grazynski, L.; Olmstead, M. M.; Balch, A. L. *Inorg. Chem.* **1997**, *36*, 4548–4554. (f) Stibrany, R. T.; Vasudevan, J.; Knapp, S.; Potenza, J. A.; Emge, T.; Schugar, H. J. *J. Am. Chem. Soc.* **1996**, *118*, 3980–3981. (g) Stang, P. J.; Fan, J.; Olenyuk, B. *Chem. Commun.* **1997**, 1453–1454. (h) Slone, R. V.; Hupp, J. T. *Inorg. Chem.* **1997**, *36*, 5422–5423. (i) Drain, C. M.; Nifiatis, F.; Vasenko, A.; Batteas, J. D. *Angew. Chem., Int. Ed.* **1998**, *37*, 2344–2347. (j) Belanger, S.; Hupp, J. T. *Angew. Chem., Int. Ed.* **1999**, *38*, 2222–2224. (k) Belanger, S.; Hupp, J. T.; Stern, C. L.; Slone, R. V.; Watson, D. F.; Carrell, T. G. *J. Am. Chem. Soc.* **1999**, *121*, 557–563. (l) Ogawa, K.; Kobuke, Y. *Angew. Chem., Int. Ed.* **2000**, *39*, 4070–4073. (m) Fujita, N.; Biradha, K.; Fujita, M.; Sakamoto, S.; Yamaguchi, K. *Angew. Chem., Int. Ed.* **2001**, *40*, 1718–1721. (n) Merlau, M. L.; Mejia, M. del, P.; Nguyen, S.; Hupp, J. T. *Angew. Chem., Int. Ed.* **2001**, *40*, 4239–4242. (o) Iengo, E.; Zangrando, E.; Minatel, R.; Alessio, E. *J. Am. Chem. Soc.* **2002**, *124*, 1003–1013. (p) Mines, G. A.; Tzeng, B.-C.; Stevenson, K. J.; Li, J.; Hupp, J. T. *Angew. Chem., Int. Ed.* **2002**, *41*, 154–157. (q) Takahashi, R.; Kobuke, Y. *J. Am. Chem. Soc.* **2003**, *125*, 2372–2373. (r) Tsuda, A.; Sakamoto, S.; Yamaguchi, K.; Aida, T. *J. Am. Chem. Soc.* **2003**, *125*, 15722–15723. (s) Suzuki, M.; Tsuge, K.; Sasaki, Y.; Imamura, T. *Chem. Lett.* **2003**, *32*, 564–565. (t) Tominaga, M.; Suzuki, K.; Kawano, M.; Kusukawa, T.; Ozeki, T.; Sakamoto, S.; Yamaguchi, K.; Fujita, M. *Angew. Chem., Int. Ed.* **2004**, *43*, 5621–5625. (u) Shoji, O.; Okada, S.; Satake, A.; Kobuke, Y. *J. Am. Chem. Soc.* **2005**, *127*, 2201–2210. (v) Tsuda, A.; Hu, H.; Tanaka, R.; Aida, T. *Angew. Chem., Int. Ed.* **2005**, *44*, 4884–4888. (w) Prodi, A.; Chiorboli, C.; Scandola, F.; Iengo, E.; Alessio, E.; Dobrawa, R.; Würthner, F. *J. Am. Chem. Soc.* **2005**, *127*, 1454–1462.
(8) (a) Tsuda, A.; Nakamura, T.; Sakamoto, S.; Yamaguchi, K.; Osuka, A. *Angew. Chem., Int. Ed.* **2002**, *41*, 2817–2821. (b) Hwang, I.-W.; Kamada, T.; Ahn, T. K.; Ko, D. M.; Nakamura, T.; Tsuda, A.; Osuka, A.; Kim, D. *J. Am. Chem. Soc.* **2004**, *126*, 16187–16198.
(9) Yoshida, N.; Ishizuka, T.; Youfu, K.; Murakami, M.; Miyasaka, H.; Okada, T.; Nagata, Y.; Itaya, A.; Cho, H. S.; Kim, D.; Osuka, A. *Chem. Eur. J.* **2003**, *9*, 2854–2866.

upfield shifts for the imide protons at 6.29 (H^c), 3.58 (H^a), and 2.65 (H^b) ppm, which indicates the coordination of the pyridyl group to Zn(II) porphyrin (Figure 1b). On the other hand, the ^{1}H NMR spectrum **2** in coordinating pyridine-d_5 exhibits corresponding peaks at normal chemical shifts; 9.69 (H^a), 9.36 (H^c), and 8.17 (H^b) ppm (Figure 1a). This observation indicates that **2** exists as a monomeric porphyrin in pyridine. X-ray-quality crystals of **2** were grown by vapor diffusion of acetonitrile into its toluene solution. The crystal system is rhombohedral and the cell volume is 27150(2) Å^3. The crystal structure revealed a triangular complex formed by complementary coordination of the cinchomeronimide group to the Zn(II) atom with a dihedral angle of 61° between the porphyrin mean planes (Figure 2).[10] The pyridyl group is coordinated to the Zn center with an angle of 88.8° and the Zn center is displaced 0.272 Å out of the N4 plane that is slightly domed.

Next, *meso—meso* linked diporphyrin **7** bearing two cinchomeronimide groups at 10,10′-positions was prepared from 5,10-bis(3,5-di-*tert*-butylphenyl)porphyrin **3** as shown in Scheme 2. Porphyrin **3** was coupled with AgPF$_6$ to give *meso—meso* linked diporphyrin[11] **4** in 17% yield, which was nitrated with AgNO$_2$ in CHCl$_3$ to afford **5** in 85% yield. Nitro groups of **5** were reduced with Pd-charcoal and NaBH$_4$ to provide 10,10′-diamino *meso—meso* linked Zn(II) diporphyrin **6** in 87% yield. Final condensation of **6** with cinchomeronic anhydride was performed in pyridine under reflux conditions for 12 h to furnish 10,10′-cinchomeronimide-appended *meso—meso* linked Zn(II) diporphyrin **7**. Importantly, a free rotation of the cinchomeronimide group is considerably restricted due to the steric hindrance of the two imide-carbonyl groups, which gives rise to three different stable atropisomers (in—in, in—out, and out—out) with respect to the orientation of the nitrogen atom in the pyridine moiety. This has been confirmed by detailed ^{1}H NMR examinations of separated conformational isomers of **7**, as explained in a later section. In addition, a free rotation around the *meso—meso* linkage is severely prohibited,[8,12] thus making all the isomers to be chiral (*R* and *S*). Therefore, six isomers are present in a solution of **7**; *R*-**7**$_{in-in}$, *S*-**7**$_{in-in}$, *R*-**7**$_{in-out}$, *S*-**7**$_{in-out}$, *R*-**7**$_{out-out}$, and *S*-**7**$_{out-out}$ (Scheme 3).

Structures of Aggregates. In noncoordinating solvents like CDCl$_3$, the ^{1}H NMR spectrum of **7** displays distinct three entities, featuring the protons of the pyridyl groups in the range of 2.9–6.5 ppm as sharp peaks (Figure 3a). This observation suggested that all the pyridyl groups in **7** are bound on Zn(II) atoms of the other molecules of **7**, probably forming three different cyclic aggregates with complementary coordination. Gel permeation chromatography (GPC) of this mixture revealed distinct three fractions (I, II, and III) in a ratio of ca. 1:2:1 in the order of increasing molecular weight. GPC analysis with polystyrene standards indicated the molecular weights of the fractions I, II, and III to be 4.8×10^3, 6.1×10^3, and 7.6×10^3 Da, which roughly correspond to trimeric, tetrameric, and pentameric aggregates of **7**, respectively. These three fractions were actually separated by preparative GPC–HPLC in 17, 34, and 16% isolated yields, respectively, on the basis of the amount of **6** used.

(10) Crystal data for **2**, (*R*-**7**$_{in-in}$)$_3$ and (*R*-**7**$_{out-out}$)$_5$: See Table 1 and SI.
(11) Nakamura, Y.; Hwang, I.-W.; Aratani, N.; Ahn, T. K.; Ko, D. M.; Takagi, A.; Kawai, T.; Matsumoto, T.; Kim, D.; Osuka, A. *J. Am. Chem. Soc.* **2005**, *127*, 236–246.
(12) Yoshida, N.; Osuka, A. *Tetrahedron Lett.* **2000**, *41*, 9287–9291.
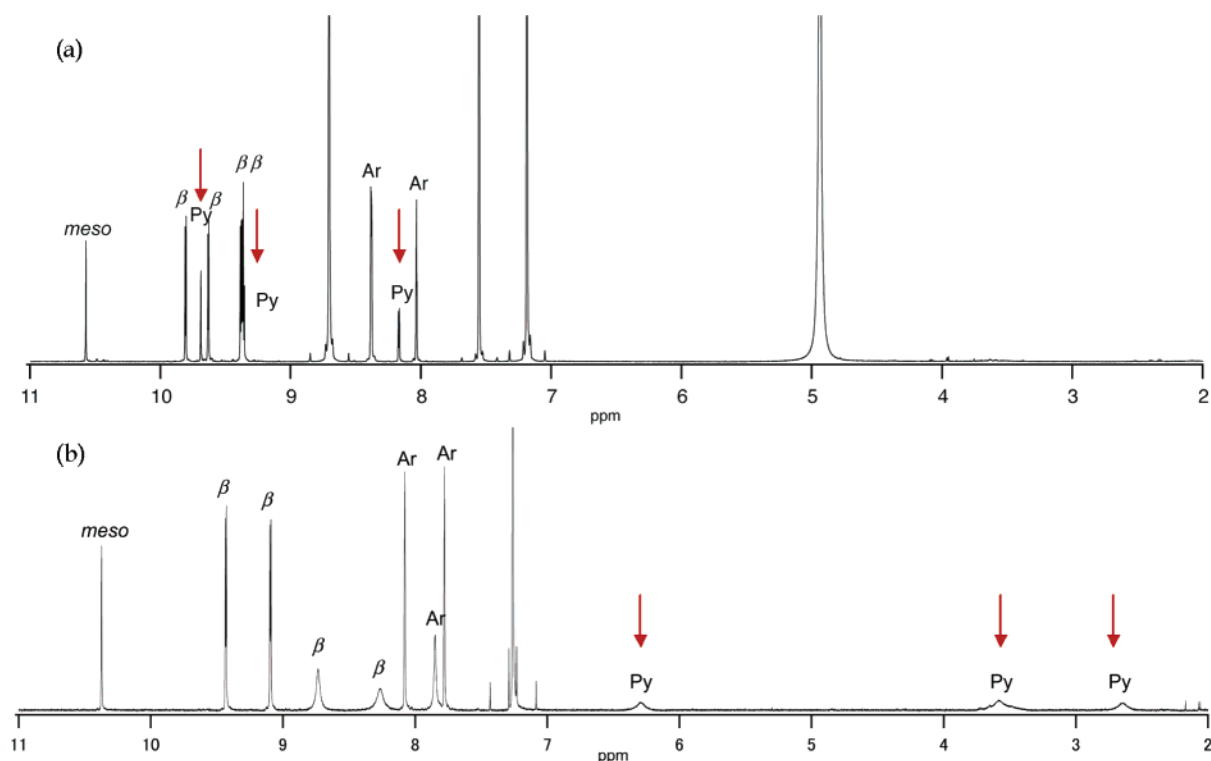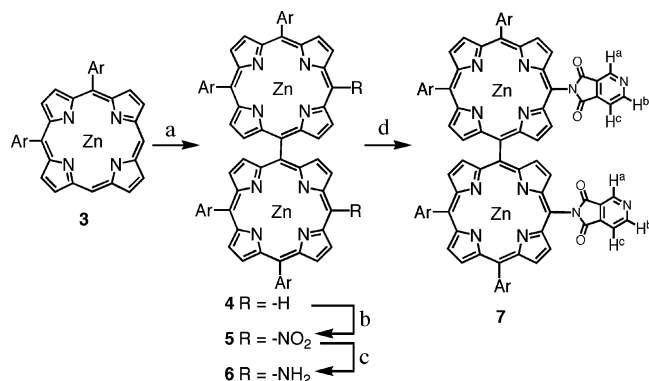
Figure 1. ¹H NMR spectra of **2** (a) in pyridine-*d*₅ and (b) in CDCl₃. Arrows indicate the pyridyl protons.
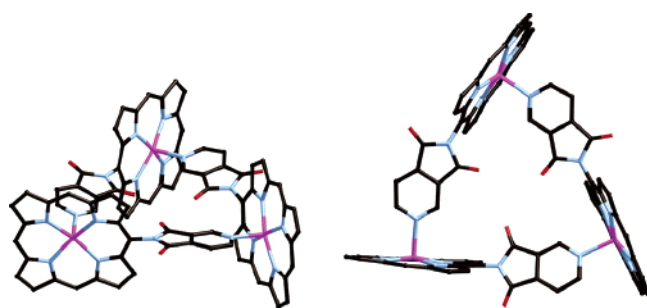
Figure 2. X-ray crystal structure of (**2**)₃. Solvent molecules, hydrogen atoms, and *meso*-aryl groups are omitted for clarity.

Scheme 2

4 R = -H
5 R = -NO₂
6 R = -NH₂

a AgPF₆, CHCl₃, 17%. *b* AgNO₂, I₂, CHCl₃, 85%. *c* NaBH₄, Pd/C, CH₂Cl₂, MeOH, 87%. *d* Cinchomeronic anhydride, pyridine, reflux, 67%. Ar = 3,5-di-*tert*-butylphenyl.

¹H NMR spectra of the fractions I, II, and III are different from one another, exhibiting the pyridyl protons; H^c at 6.49 ppm, H^a at 4.03 ppm, and H^b at 2.94 ppm for the fraction I, H^c at 6.52 and 6.16 ppm, H^a at 3.82 and 3.15 ppm, H^b at 3.29 and 3.15 ppm for the fraction II, and H^c at 6.15 ppm, H^a at 3.90

ppm, and H^b at 2.95 ppm for the fraction III, respectively (Figures 3b–d). It is important to note that only single sets of the signals were observed for the fractions I and III, while two sets of the signals were detected for the fraction II. ¹H NMR spectrum of as prepared **7** is a simple sum of those of the fractions I, II, and III in a ratio of ca. 1:2:1, indicating that these aggregates are stable in CDCl₃ solution and there is no scrambling of diporphyrin fragments. When these aggregates were dissolved in pyridine-*d*₅, their ¹H NMR spectra became very similar and exhibited the pyridyl protons without no particular upfield shifts, indicating their dissociation. As discussed in a later section, the dissociation of **7** in pyridine has been supported also by the absorption spectra and CD spectra. The ¹H NMR spectra of the fractions I, II, and III were similar but were distinctly different from one another, particularly in the chemical shifts of the protons due to the inner β-protons near the imide group (Supporting Information; SI), which has been interpreted to indicate that the three aggregates consist of respective different diporphyrin conformers. Most probably, the three conformers can be assigned as **7**$_{in-in}$, **7**$_{in-out}$, and **7**$_{out-out}$, (Scheme 3). These isomers are conformationally rather stable, as shown by heating experiments (110 °C, 24 h, in pyridine) of these separated conformers that led to only ca. 10% isomerization.

Despite many attempts to determine the molecular weights of the fractions I, II, and III, their parent ion peaks as aggregates could not be detected either by MALDI-TOF, FAB, or cold-spray ionization mass techniques. Thus, we attempted X-ray diffraction analysis of these aggregates. In the course of these attempts, we found that chiral separation of the fraction I was possible through a chiral HPLC column (SI) and reasonably nice crystals of the fraction I were obtained by slow diffusion of acetonitrile into a toluene solution of the chiral fraction I. X-ray diffraction analysis on this crystal provided preliminary

Scheme 3. Schematic Representation of Self-Sorting Process of Diporphyrins
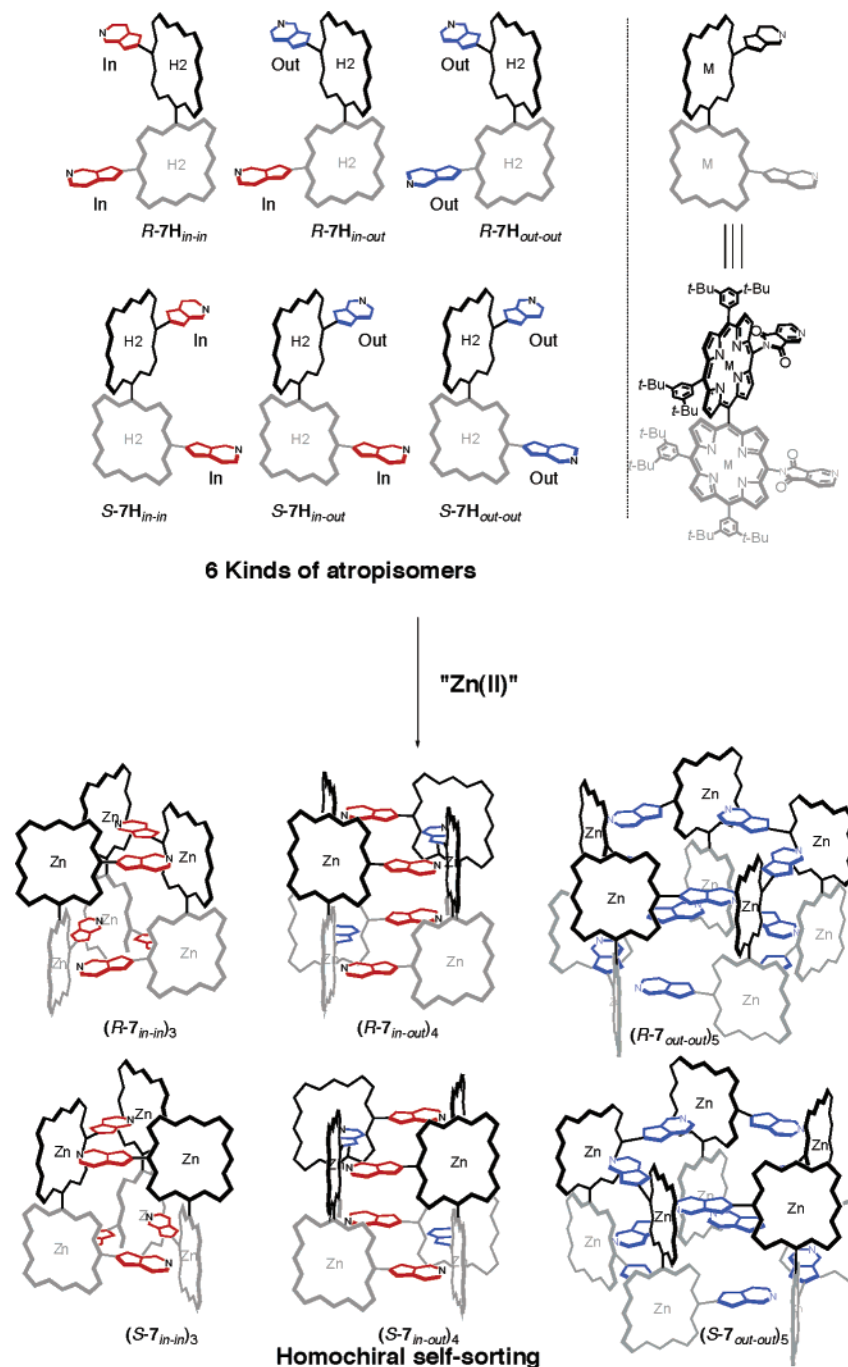
data, which indicated a pair of trimers in the unit cell. Each trimer was constructed by complementary coordination of three molecules of an in-in conformer (R-7_{in-in}) (SI). Largely due to the disorder of many solvent molecules contained in the crystal, the X-ray data remain preliminary level but the main skeletal structure should be certain. As more convincing information, we have succeeded in X-ray crystal diffraction analysis of the fraction III. After many attempts, X-ray-quality crystals were obtained by slow diffusion of acetonitrile into a toluene solution of optically pure R-$7_{out-out}$.[13] X-ray diffraction data set for (R-$7_{out-out}$)$_5$ was collected with 44571 unique reflections ($>2\sigma(I)$) at BL44B2 beamline of SPring-8 Japan.[10] The crystal system

is monoclinic and the cell volume is quite large, 46060(8) Å³. The crystal structure thus determined shows a symmetric pentameric aggregate consisting of five molecules of R-$7_{out-out}$ (Figure 4). The aggregate (R-$7_{out-out}$)$_5$ exhibits a C_5 symmetric pentagonal cylindrical structure with sides of ca. 11.5 Å and internal angles of ca. 108°. In the crystal, the aggregates (R-$7_{out-out}$)$_5$ are stacked in a tubular manner to form an infinite channel of ca. 10 Å diameter (Figure 5). Each pentagonal channel unit contacts through CH-π interactions between 3,5-di-*tert*-butylphenyl groups and Zn(II) porphyrin planes to form a linear zigzag network (Figure 5c). Then, the fraction II has been rationally assigned as a tetrameric aggregate (7)$_4$ composed of four molecules of an in−out conformer (R-7_{in-out}) on the basis of its GPC retention time that indicated its molecular size

(13) Diporphyrin **4** was separated into R-**4** and S-**4**, and R-**4** was converted to R-**7** via the same synthetic route.
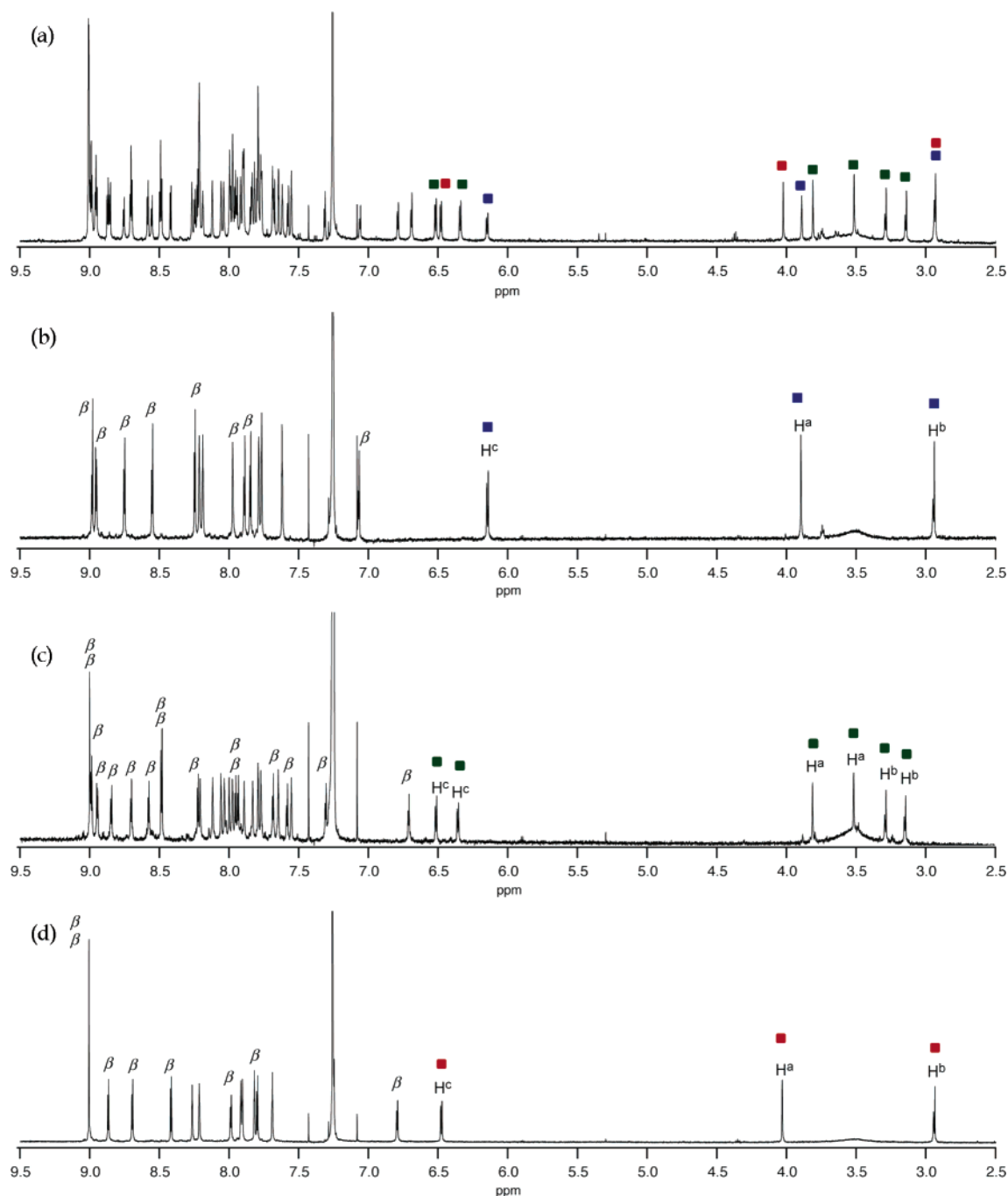
Figure 3. ^{1}H NMR spectra of as prepared **7** (a), and of the fractions III, II, and I, ((b), (c), and (d)) in CDCl$_3$. The fractions III, II, and I have been assigned as $(\mathbf{7}_{out-out})_5$, $(\mathbf{7}_{in-out})_4$, and $(\mathbf{7}_{in-in})_3$, respectively. See the discussion in the text.

to be larger than $(\mathbf{7})_3$ and smaller than $(\mathbf{7})_5$. Cyclic symmetric structures of $(\mathbf{7})_3$ and $(\mathbf{7})_5$ well explain their ^{1}H NMR data showing single sets of signals due to the pyridyl protons, since all the constitutional diporphyrins are identical. On the other hand, the observed two sets of signals due to the pyridyl protons in a 1:1 ratio in the ^{1}H NMR of $(\mathbf{7})_4$ can be explained by the presence of the inward and outward orientating pyridyl protons.

Energy minimized structures of $(R\text{-}\mathbf{7}'_{in-in})_3$, $(R\text{-}\mathbf{7}'_{in-out})_4$, and $(R\text{-}\mathbf{7}'_{out-out})_5$ were calculated by the DFT method in which *meso* 3,5-di-*tert*-butylphenyl substituents of **7** are replaced by hydrogen (Figure 6). Calculated structures for $(R\text{-}\mathbf{7}'_{in-in})_3$ and $(R\text{-}\mathbf{7}'_{out-out})_5$ were almost exactly the same as those of the corresponding X-ray structures, in which the pyridyl nitrogen

atoms are coordinated to the Zn(II) atoms with angles of N–Zn and porphyrin 24 core atoms plane 88 and 85° for $(R\text{-}\mathbf{7}'_{in-in})_3$ and $(R\text{-}\mathbf{7}'_{out-out})_5$ respectively. On the other hand, a quadratic prismatic structure was calculated for $(R\text{-}\mathbf{7}'_{in-out})_4$, in which four molecules of $\mathbf{7}'_{in-out}$ assembled by an alternate in- and out-pyridyl coordination with angles of N–Zn and porphyrin 24 core atoms plane, 89 and 86° for *inward*- and *outward*-oriented cinchomeronimides. The calculated structure of $(R\text{-}\mathbf{7}'_{in-out})_4$ well explains the ^{1}H NMR spectrum, since all the inward- and outward-orientating pyridyl groups are respectively identical in the aggregate.

UV–Vis Absorption Spectra. Figure 7 shows the absorption spectra of $(R\text{-}\mathbf{7}_{in-in})_3$, $(R\text{-}\mathbf{7}_{in-out})_4$, and $(R\text{-}\mathbf{7}_{out-out})_5$ in pyridine
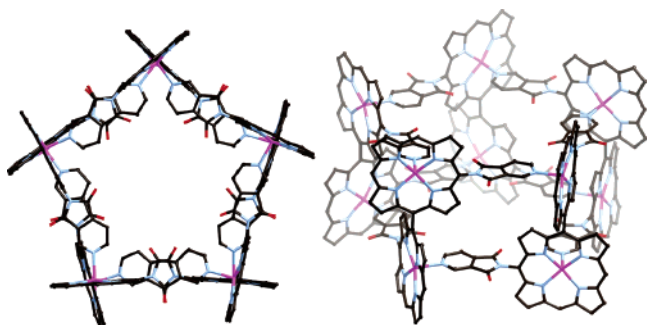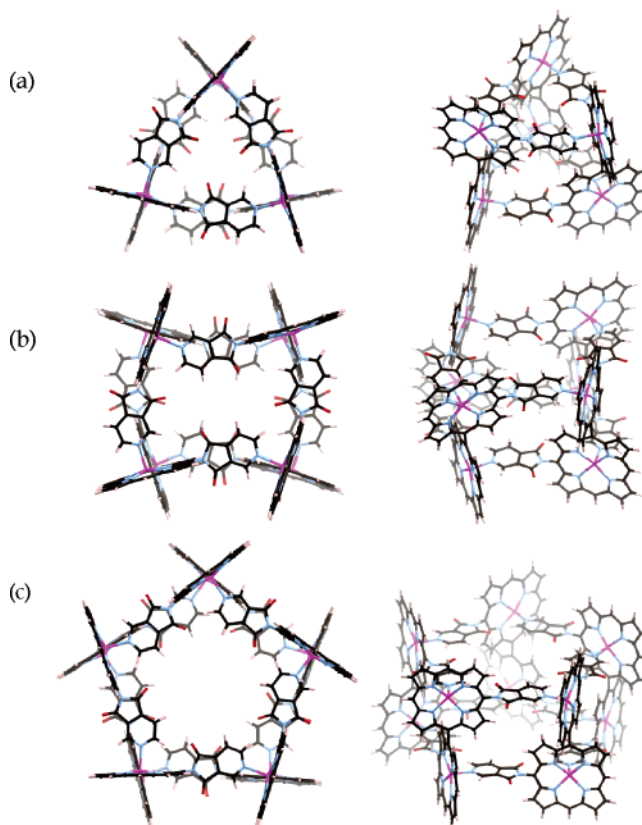
Figure 4. X-ray crystal structure of (R-$7_{out-out}$)$_5$; top view (left) and side view (right). Solvent molecules, hydrogen atoms, and *meso*-aryl groups are omitted for clarity.
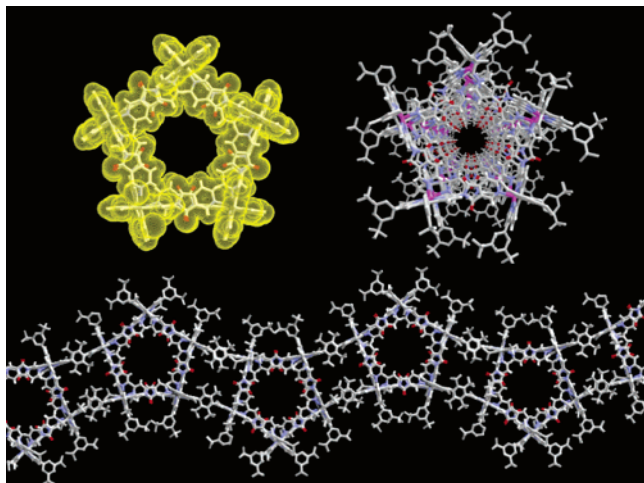
Figure 5. van der Waals structure (top, left) and packing diagram for (R-$7_{out-out}$)$_5$; perspective view (top, right) and top view (bottom). Solvent molecules and hydrogen atoms on *tert*-butyl groups are omitted for clarity.

(a) and in CHCl$_3$ (b). It has been known that the exciton coupling in the Soret band of *meso*−*meso* linked diporphyrins is sensitive to the dihedral angle between the porphyrins.[14] The absorption spectra in pyridine are practically the same for the three samples, exhibiting split Soret bands due to the exciton coupling between the porphyrin units.[15] The observed splitting widths are all ca. 1960 cm^{-1}, which are typical for free *meso*−*meso* linked zinc-(II) diporphyrins having wide distribution of dihedral angle between the two porphyrins. On the other hand, the absorption spectra of (R-7_{in-in})$_3$, (R-7_{in-out})$_4$, and (R-$7_{out-out}$)$_5$ in CHCl$_3$ are different from one another, which is caused by different exciton coupling in each aggregate (Figure 7b). The observed narrow splitting widths in the spectra in CHCl$_3$ (1540, 1390, and 1290 cm^{-1} for (R-7_{in-in})$_3$, (R-7_{in-out})$_4$, and (R-$7_{out-out}$)$_5$, respectively) has been interpreted in terms of considerably reduced conformational freedom of the diporphyrin segments in the aggregates.[8]

Chiral Separation, CD Spectra, and Association Constants. Since conformational isomers of **7** (**7**$_{in-in}$, **7**$_{in-out}$, and **7**$_{out-out}$) are all chiral, the aggregates (**7**$_{in-in}$)$_3$, (**7**$_{in-out}$)$_4$, and

(14) (a) Yoshida, N.; Ishizuka, T.; Osuka, A.; Jeong, D. H.; Cho, H. S.; Kim, D.; Matsuzaki, Y.; Nogami, A.; Tanaka, K. *Chem. Eur. J.* **2003**, *9*, 58−75. (b) Jeong, D. H.; Jang, S. M.; Hwang, I.-W.; Kim, D.; Yoshida, N.; Osuka, A. *J. Phys. Chem. A* **2002**, *106*, 11054−11063.
(15) (a) Aratani, N.; Osuka, A.; Kim, Y. H.; Jeong, D. H.; Kim, D. *Angew. Chem., Int. Ed.* **2000**, *39*, 1458−1462. (b) Aratani, N.; Takagi, A.; Yanagawa, Y.; Matsumoto, T.; Kawai, T.; Yoon, Z. S.; Kim, D.; Osuka, A. *Chem. Eur. J.* **2005**, *11*, 3389−3404.

Figure 6. DFT calculated structures of (a) (R-$7'_{in-in}$)$_3$, (b) (R-$7'_{in-out}$)$_4$, and (c) (R-$7'_{out-out}$)$_5$.

(**7**$_{out-out}$)$_5$ that are formed via homochiral self-sorting of respective R- or S-enantiomer of **7**$_{in-in}$, **7**$_{in-out}$, and **7**$_{out-out}$ should be all chiral. Among these aggregates, (**7**$_{in-in}$)$_3$ was actually separated into (R-7_{in-in})$_3$ and (S-7_{in-in})$_3$ through a chiral HPLC column. In an alternate route, the optically pure aggregates (R-7_{in-in})$_3$, (R-7_{in-out})$_4$, and (R-$7_{out-out}$)$_5$, and (S-7_{in-in})$_3$, (S-7_{in-out})$_4$, and (S-$7_{out-out}$)$_5$ were constructed from preseparated optically pure diporphyrins R-**7** and S-**7**, respectively, and were separated by preparative GPC−HPLC. Three sets of (R-7_{in-in})$_3$ and (S-7_{in-in})$_3$, (R-7_{in-out})$_4$ and (S-7_{in-out})$_4$, and (R-$7_{out-out}$)$_5$ and (S-$7_{out-out}$)$_5$ are identical to their respective racemic mixtures in terms of the ^{1}H NMR and absorption spectra, while the circular dichroism (CD) spectra in CHCl$_3$ exhibit different strong Cotton effects depending on the ring size (3, 4, and 5) respectively and are perfect mirror images to each other (Figure 8 and SI). In pyridine, the optically pure aggregates (**7**$_{in-in}$)$_3$, (**7**$_{in-out}$)$_4$, and (**7**$_{out-out}$)$_5$ are all completely dissociated, as seen from their weak and reverse Cotton effects compared with those in CHCl$_3$.

The association constants of (**7**$_{in-in}$)$_3$ and (**7**$_{out-out}$)$_5$ have been estimated to be both very large, $> 10^{18}$ M^{-2} and $> 10^{27}$ M^{-4}, respectively, irrespective of racemic or optically pure precursors on the basis of concentration independence of their absorption spectra up to rather high dilution ($\sim 10^{-7}$ M). This can be explained by highly complementary and multipoint interactions without significant strain. On the other hand, the association behavior of **7**$_{in-out}$ depends on precursor, either optically pure or racemic. The association constant of optically pure R-**7**$_{in-out}$ was estimated to be certainly large as much as 2.0×10^{16} M^{-3}, but the UV−vis titration curve for the association of racemic **7**$_{in-out}$ was complicated, which precluded precise estimation of

Figure 7. UV−vis absorption spectra of (R-$7_{out-out}$)$_5$, (R-$7_{int-out}$)$_4$ and (R-7_{in-in})$_3$ in pyridine (a) and in CHCl$_3$ (b).

Figure 8. CD spectra of R-7 (a) in CHCl$_3$ and (b) in pyridine.

the association constant. These results indicate weaker complementary coordination interaction and hence imperfect enantiomeric self-sorting for 7_{in-out}.

Summary. We have demonstrated that the *meso*-cinchomeronimide appended Zn(II) porphyrin **2** forms a cyclic trimer, while the diporphyrins **7** exhibit high-fidelity self-sorting assembling to form discrete cyclic trimer, tetramer, and pentamer with large association constants from 7_{in-in}, 7_{in-out}, and $7_{out-out}$, respectively, through almost perfect discrimination of enantiomeric and conformational differences of the *meso*-cinchomeronimide substituents. In the latter self-sorting processes, the dihedral angles dictated by the two pyridyl nitrogen atoms control the size of the aggregates; the trimer from 7_{in-in}, the tetarmer from 7_{in-out}, and the pentamer from $7_{out-out}$. Exclusive formation of the discrete cyclic aggregates without no appreciable amount of polymeric aggregate is also notable, which is probably driven by favorable entropic factors for the formation of cyclic aggregates. As such, *meso−meso* linked diporphyrins are interesting and unique structural platforms that provide large discrete cyclic constructs via unique self-sorting assembling process. Exploration of even larger discrete porphyrin rings with appropriate optical functions will be the subject of further investigation.

Experimental Section

All reagents and solvents were of the commercial reagent grade and were used without further purification except where noted. Dry CHCl$_3$ were obtained by distilling over CaH$_2$. Spectroscopic grade CHCl$_3$ and pyridine were used as solvents for all spectroscopic studies. ^{1}H NMR spectra were recorded on a JEOL ECA-delta-600 spectrometer, and chemical shifts were reported as the delta scale in ppm relative to CHCl$_3$ (δ = 7.260 ppm) or pyridine (δ = 8.71 ppm). UV−vis absorption spectra were recorded on a Shimadzu UV-3100 spectrometer. Mass spectra were recorded on a JEOL HX-110 spectrometer, using positive-FAB ionization method with accelerating voltage 10 kV and a 3-nitrobenzyl alcohol matrix, and on a Shimadzu KRATOS KOMPACT MALDI 4 spectrometer, using positive-MALDI ionization method with/without 9-nitroanthracene (9NA) matrix. All theoretical calculations were carried out using the *Gaussian 03* program.[16] Initial structures of aggregates, where *meso*-aryl groups were omitted and replaced with hydrogen atoms, were obtained through optimization with the AM1 Hamiltonian. All structures were then optimized with Becke's three-parameter hybrid exchange functional and the Lee−Yang−Parr correlation functional (B3LYP), employing the LANL2DZ basis set for zinc atom, and 3-21G* basis set for the other atom.

Zn(II) 10-Cinchomeronimide-5,15-bis(3,5-di-*tert*-butylphenyl)-porphyrin 2. A solution of Zn(II) 5-amino-10,20-bis(3,5-di-*tert*-butylphenyl)porphyrin **1** (40 mg, 0.054 mmol) and cinchomeronic anhydride (80 mg, 0.54 mmol) in pyridine (20 mL) was heated under

reflux for 14 h. After removal of the solvent, the residue was separated over a silica gel column with a mixture of THF and hexane to give **2** (25 mg, 0.028 mmol, 52%); ^{1}H NMR (CDCl$_3$) δ 10.37 (s, 1H, Por-*meso*), 9.42 (d, $J = 5$ Hz, 2H, Por-β), 9.09 (d, $J = 5$ Hz, 2H, Por-β), 8.73 (br, 2H, Por-β), 8.25 (br, 2H, Por-β), 8.08 (s, 2H, Ar), 7.85 (s, 2H, Ar), 7.78 (s, 2H, Ar), 6.29 (br, 1H, Py), 3.58 (br, 1H, Py), 2.65 (br, 1H, Py), 1.63 (s, 18H, *t*-Bu), and 1.46 ppm (s, 18H, *t*-Bu); UV−vis (CHCl$_3$) $\lambda_{max} = 420$ and 548 nm; FAB−MS $m/z = 894.35$, calcd. for C$_{55}$H$_{54}$N$_6$O$_2$Zn $m/z = 894.36$.

Meso-meso **Linked Zn(II) Diporphyrin 4.** A stock solution of AgPF$_6$ in dry CH$_3$CN (0.12 M, 1.85 mL) was added to a solution of Zn(II) 5,10-bis(3,5-di-*tert*-butylphenyl) porphyrin **3** (300 mg, 0.400 mmol) in dry CHCl$_3$ (270 mL), and the resulting mixture was stirred for 1 h at 5 °C in the dark. The reaction was stopped by washing with water and the organic layer was dried over anhydrous Na$_2$SO$_4$. The solvent was removed by a rotary evaporator and the residue was separated by a preparative size exclusion column with CHCl$_3$ as an eluent. Zn(II) diporphyrin **4** was obtained after recrystallization from CH$_2$Cl$_2$/hexane (53 mg, 17%); ^{1}H NMR (CDCl$_3$) δ 10.33 (s, 2H, Por-*meso*), 9.48 (d, $J = 5$ Hz, 2H, Por-β), 9.24 (d, $J = 4$ Hz, 2H, Por-β), 9.15 (d, $J = 5$ Hz, 2H, Por-β), 9.15 (d, $J = 5$ Hz, 2H, Por-β), 9.08 (d, $J = 5$ Hz, 2H, Por-β), 8.73 (d, $J = 5$ Hz, 2H, Por-β), 8.29 (d, $J = 5$ Hz, 2H, Por-β), 8.22 (s, 2H, Ar−H), 8.20 (s, 2H, Ar−H), 8.14 (d, $J = 5$ Hz, 2H, Por-β), 8.10 (s, 2H, Ar−H), 8.09 (s, 2H, Ar−H), 7.87 (s, 2H, Ar−H), 7.69 (s, 2H, Ar−H), 1.61 (s, 18H, *t*-Bu), 1.60 (s, 18H, *t*-Bu), 1.44 (s, 18H, *t*-Bu), and 1.43 ppm (s, 18H, *t*-Bu); UV−vis (CHCl$_3$) $\lambda_{max} = 412$, 450, and 552 nm; MALDI-TOF−MS $m/z = 1498.8$, calcd. for C$_{96}$H$_{102}$N$_8$Zn$_2$ $m/z = 1498.7$.

10,10′-Dinitrated *meso−meso* **Linked Zn(II) Diporphyrin 5.** A solution of AgNO$_2$ (60 mg, 0.39 mmol) in dry CH$_3$CN (2.0 mL) was added to a solution of **4** (147 mg, 0.098 mmol) and iodine (100 mg, 0.39 mmol) in CHCl$_3$ (30 mL). After refluxing for 10 min, the reaction mixture was washed with water, aqueous Na$_2$S$_2$O$_4$, water and brine, and was dried over anhydrous Na$_2$SO$_4$. The solvent was removed by a rotary evaporator and the residue was separated by silica gel column chromatography with a mixture of CH$_2$Cl$_2$ and hexane. A solution of Zn(OAc)$_2$ in the methanol was added to a solution of the separated compound in CH$_2$Cl$_2$. After stirring for 1 h, the solution was washed with water and dried over anhydrous Na$_2$SO$_4$. The solvent was removed by a rotary evaporator to give **5** (132 mg, 85%); ^{1}H NMR (CDCl$_3$) δ 9.24 (br, 2H, Por-β), 9.14 (d, $J = 5$ Hz, 2H, Por-β), 9.04 (d, $J = 5$ Hz, 2H, Por-β), 9.02 (d, $J = 5$ Hz, 2H, Por-β), 8.92 (br, 2H, Por-β), 8.67 (d, $J = 5$ Hz, 2H, Por-β), 8.24 (d, $J = 5$ Hz, 2H, Por-β), 8.19 (br, 2H, Ar), 8.11 (br, 2H, Ar), 8.07 (br, 2H, Ar), 8.02 (br, 2H, Ar), 7.97 (d, $J = 5$ Hz, 2H, Por-β), 7.89 (t, $J = 2$ Hz, 2H, Ar), 7.71 (t, $J = 2$ Hz, 2H, Ar), 1.62 (s, 18H, *t*-Bu), 1.59 (s, 18H, *t*-Bu), 1.47 (s, 18H, *t*-Bu), and 1.43 ppm (s, 18H, *t*-Bu); UV−vis (CHCl$_3$) $\lambda_{max} = 412$, 450, and 552 nm; MALDI-TOF−MS $m/z = 1588.5$, calcd. for C$_{96}$H$_{100}$N$_{10}$O$_4$Zn$_2$ $m/z = 1588.7$.

10,10′-Diaminated *meso−meso* **Linked Zn(II) Diporphyrin 6.** Diporphyrin **5** (75 mg, 0.047 mmol) was dissolved in CH$_2$Cl$_2$ (30 mL) and methanol (30 mL), to which 10% Pd/carbon (50 mg) was added. Then, NaBH$_4$ (36 mg, 0.94 mmol) was added to the solution, and the resulting reaction mixture was stirred for 20 min at room temperature. Pd/carbon was filtered off and the filtrate was washed with water and the organic layer was dried over anhydrous Na$_2$SO$_4$. The solvent was removed by a rotary evaporator and the residue was separated by silica gel chromatography with CH$_2$Cl$_2$ to give **6** (63 mg, 87%); ^{1}H NMR (pyridine-d_5) δ 9.89 (d, $J = 4$ Hz, 2H, Por-β), 9.51 (d, $J = 5$ Hz, 2H, Por-β), 9.04 (br, 4H, NH$_2$), 8.92 (m, 4H, Por-β), 8.11 (d, $J = 5$ Hz, 2H, Por-β), 8.59 (d, $J = 5$ Hz, 2H, Por-β), 8.39 (s, 2H, Ar), 8.36 (s, 2H, Ar), 8.33 (s, 2H, Ar), 8.29 (s, 2H, Ar), 8.23 (d, $J = 5$ Hz, 2H, Por-β), 8.05 (d, $J = 4$ Hz, 2H, Por-β), 8.00 (s, 2H, Ar), 7.84 (s, 2H,

Ar), 1.53 (s, 18H, *t*-Bu), 1.44 (s, 9H, *t*-Bu), and 1.43 ppm (s, 9H, *t*-Bu); UV−vis (pyridine) $\lambda_{max} = 440$, 462, and 683 nm; MALDI−TOF-MS $m/z = 1527.9$, calcd. for C$_{96}$H$_{104}$N$_{10}$Zn$_2$ $m/z = 1528.7$.

10,10′-Bis(cinchomeronimide)-Appended *meso−meso* **Linked Zn-(II) Diporphyrin 7 and its Separation to (7$_{out−out}$)$_5$, (7$_{in−out}$)$_4$ and (7$_{in−in}$)$_3$.** A solution of **6** (45 mg, 0.029 mmol) and cinchomeronic anhydride (132 mg, 0.883 mmol) in pyridine (20 mL) was heated under reflux for 12 h. After the removal of the solvent, the residue was purified over a silica gel column with THF/hexane. The solvent was removed by a rotary evaporator and the residue was separated by a size exclusion column chromatography with CHCl$_3$ as an eluent to give (7$_{out−out}$)$_5$ (8.5 mg, 16%), (7$_{in−out}$)$_4$ (18.1 mg, 34%) and (7$_{in−in}$)$_3$ (9.1 mg, 17%).

(7$_{out−out}$)$_5$. ^{1}H NMR (CDCl$_3$) δ 8.98 (d, $J = 4$ Hz, 2H, Por-β), 8.96 (d, $J = 4$ Hz, 2H, Por-β), 8.76 (d, $J = 4$ Hz, 2H, Por-β), 8.56 (d, $J = 5$ Hz, 2H, Por-β), 8.28 (d, $J = 5$ Hz, 2H, Por-β), 8.22 (br, 2H, Ar), 8.2 (br, 2H, Ar), 7.98 (br, 2H, Ar), 7.9 (d, $J = 4$ Hz, 2H, Por-β), 7.85 (d, $J = 4$ Hz, 2H, Por-β), 7.79 (br, 2H, Ar), 7.77 (br, 2H, Ar), 7.63 (t, $J = 2$ Hz, 2H, Ar), 7.08 (d, $J = 4$ Hz, 2H, Por-β), 6.15 (d, $J = 6$ Hz, 2H, Py), 3.90 (s, 2H, Py), 2.95 (d, $J = 6$ Hz, 2H, Py), 1.61 (s, 18H, *t*-Bu), 1.46 (s, 18H, *t*-Bu), 1.35 (s, 18H, *t*-Bu), and 1.31 ppm (s, 18H, *t*-Bu); ^{1}H NMR (pyridine-d_5) δ 9.80 (d, $J = 4$ Hz, 2H, Por-β), 9.57 (s, 2H, Py), 9.45 (d, $J = 4$ Hz, 2H, Por-β), 9.43 (d, $J = 4$ Hz, 2H, Por-β), 9.33 (m, 4H, Por-β + Py), 9.20 (d, $J = 5$ Hz, 2H, Por-β), 8.97 (d, $J = 4$ Hz, 2H, Por-β), 8.53 (br, 2H, Ar), 8.51 (br, 2H, Ar), 8.50 (br, 2H, Ar), 8.48 (br, 2H, Ar), 8.19 (d, $J = 4$ Hz, 2H, Por-β), 8.07 (d, $J = 4$ Hz, 2H, Por-β), 8.06 (br, 2H, Ar), 8.03 (d, $J = 6$ Hz, 2H, Py), 7.98 (t, $J = 2$ Hz, 2H, Ar), 1.56 (s, 18H, *t*-Bu), 1.55 (s, 18H, *t*-Bu), 1.48 (s, 18H, *t*-Bu), and 1.47 ppm (s, 18H, *t*-Bu); UV−vis (CHCl$_3$) $\lambda_{max} = 428$, 453, and 571 nm.

(7$_{in−out}$)$_4$. ^{1}H NMR (CDCl$_3$) δ 9.00 (s, 2H, Por-β), 8.99 (d, $J = 5$ Hz, 1H, Por-β), 8.95 (d, $J = 5$ Hz, 1H, Por-β), 8.85 (d, $J = 5$ Hz, 1H, Por-β), 8.71 (d, $J = 4$ Hz, 1H, Por-β), 8.58 (d, $J = 4$ Hz, 1H, Por-β), 8.49 (d, $J = 5$ Hz, 2H, Por-β), 8.23 (d, $J = 4$ Hz, 1H, Por-β), 8.21 (br, 1H, Ar), 8.11 (br, 1H, Ar), 8.06 (br, 1H, Ar), 8.03 (br, 1H, Ar), 8.00 (br, 1H, Ar), 7.97 (br, 1H, Ar), 7.96 (d, $J = 4$ Hz, 1H, Por-β), 7.94 (d, $J = 4$ Hz, 1H, Por-β), 7.89 (br, 1H, Ar), 7.83 (br, 1H, Ar), 7.69 (d, $J = 4$ Hz, 1H, Por-β), 7.65 (t, $J = 2$ Hz, 1H, Ar), 7.59 (d, $J = 5$ Hz, 1H, Por-β), 7.55 (t, $J = 2$ Hz, 1H, Ar), 7.31 (d, $J = 4$ Hz, 1H, Por-β), 6.72 (d, $J = 5$ Hz, 1H, Por-β), 6.52 (d, $J = 6$ Hz, 1H, Py), 6.16 (d, $J = 6$ Hz, 1H, Py), 3.82 (s, 1H, Py), 3.52 (s, 1H, Py), 3.29 (d, $J = 6$ Hz, 1H, Py), 3.15 (d, $J = 6$ Hz, 1H, Py), 1.62 (s, 9H, *t*-Bu), 1.58 (s, 9H, *t*-Bu), 1.49 (s, 9H, *t*-Bu), 1.46 (s, 9H, *t*-Bu), 1.39 (s, 27H, *t*-Bu), and 1.09 ppm (s, 9H, *t*-Bu); ^{1}H NMR (pyridine-d_5) δ 9.80 (d, $J = 4$ Hz, 2H, Por-β), 9.57 (s, 2H, Py), 9.45 (d, $J = 4$ Hz, 2H, Por-β), 9.43 (d, $J = 4$ Hz, 2H, Por-β), 9.34 (m, 4H, Por-β + Py), 9.20 (d, $J = 5$ Hz, 1H, Por-β), 9.20 (d, $J = 5$ Hz, 1H, Por-β), 8.98 (d, $J = 4$ Hz, 1H, Por-β), 8.97 (d, $J = 4$ Hz, 1H, Por-β), 8.53 (br, 2H, Ar), 8.51 (br, 4H, Ar), 8.48 (br, 1H, Ar), 8.47 (br, 1H, Ar), 8.21 (d, $J = 4$ Hz, 1H, Por-β), 8.18 (d, $J = 4$ Hz, 1H, Por-β), 8.08 (d, $J = 4$ Hz, 1H, Por-β), 8.06 (br, 2H, Ar), 8.03 (d, $J = 4$ Hz, 1H, Por-β), 8.03 (d, $J = 6$ Hz, 1H, Py), 8.02 (d, $J = 6$ Hz, 1H, Py), 7.98 (t, $J = 2$ Hz, 2H, Ar), 1.56 (s, 18H, *t*-Bu), 1.55 (s, 18H, *t*-Bu), 1.49 (s, 18H, *t*-Bu), 1.48 (s, 9H, *t*-Bu), and 1.47 ppm (s, 9H, *t*-Bu); UV−vis (CHCl$_3$) $\lambda_{max} = 427$, 454, and 569 nm.

(7$_{in−in}$)$_3$. ^{1}H NMR (CDCl$_3$) δ 9.01 (s, 4H, Por-β), 8.87 (d, $J = 5$ Hz, 2H, Por-β), 8.70 (d, $J = 5$ Hz, 2H, Por-β), 8.42 (d, $J = 5$ Hz, 2H, Por-β), 8.26 (br, 2H, Ar), 8.21 (br-s, 2H, Ar), 7.99 (d, $J = 5$ Hz, 2H, Por-β), 7.92 (br, 2H, Ar), 7.91 (br, 2H, Ar), 7.82 (br, 2H, Ar), 7.80 (d, $J = 5$ Hz, 2H, Por-β), 7.69 (t, $J = 2$ Hz, 2H, Ar), 6.79 (d, $J = 5$ Hz, 2H, Por-β), 6.48 (d, $J = 6$ Hz, 2H, Py), 4.03 (s, 2H, Py), 2.94 (d, $J = 6$ Hz, 2H, Py), 1.68 (s, 18H, *t*-Bu), 1.49 (s, 18H, *t*-Bu), 1.48 (s, 18H, *t*-Bu), and 1.38 ppm (s, 18H, *t*-Bu); ^{1}H NMR (pyridine-d_5) δ 9.80 (d, $J = 4$ Hz, 2H, Por-β), 9.57 (s, 2H, Py), 9.45 (d, $J = 4$ Hz, 2H, Por-β), 9.43 (d, $J = 4$ Hz, 2H, Por-β), 9.34 (m, 4H, Por-β + Py), 9.21 (d, $J = 5$ Hz, 2H, Por-β), 8.98 (d, $J = 4$ Hz, 2H, Por-β), 8.53 (br, 2H, Ar), 8.51 (br, 4H, Ar), 8.48 (br, 2H, Ar), 8.21 (d, $J = 4$ Hz, 2H, Por-β),

(16) Frisch, M. J.; et al. *Gaussian03*, Revision B.05. Gaussian, Inc.: Pittsburgh, PA, 2003.

Table 1. Crystal Data and Structure Refinement for (**2**)$_3$ and (*R*-**7**$_{out-out}$)$_5$

	(**2**)$_3$		(*R*-**7**$_{out-out}$)$_5$	
formula	C376H324N47O17Zn6		C522 H722 N60 O20 Zn10	
formula weight	6149.04		8811.30	
temp	120(2) K		293(2) K	
wavelength	0.71073 Å		0.71073 Å	
crystal system	Rhombohedral		Monoclinic	
space group	*R*-3		*P*2$_1$	
unit cell dimensions	$a = 22.8553(7)$ Å	$\alpha = 90°$	$a = 29.95(3)$ Å	$\alpha = 90°$
	$b = 22.8553(7)$ Å	$\beta = 90°$	$b = 54.46(5)$ Å	$\beta = 111.06(5)°$
	$c = 60.016(4)$ Å	$\gamma = 120°$	$c = 30.26(3)$ Å	$\gamma = 90°$
vol	27150(2) Å^3		46060(8) Å^3	
Z	3		2	
density (calculated)	1.128 Mg/m^3		0.635 Mg/m^3	
absorption coeff	0.454 mm^{-1}		0.290 mm^{-1}	
F(000)	9651		9468	
crystal size	$0.40 \times 0.30 \times 0.10$ mm^3		$0.20 \times 0.20 \times 0.20$ mm^3	
theta range for data collection	1.08 to 28.32°		1.72 to 18.41°	
reflections collected	52174		56692	
independent reflections	13839 [R(int) = 0.0953]		44571 [R(int) = 0.3143]	
absorption correction	Empirical		Empirical	
refinement method	Full-matrix least-squares on F^2			
data/restraints/parameters	13839/15/646		56692/6191/4246	
goodness-of-fit on F^2	0.969		2.415	
final *R* indices [*I* > 2sigma(*I*)]	$R_1 = 0.0992$, $wR_2 = 0.2875$		$R_1 = 0.1147$, $wR_2 = 0.3123$	
R indices (all data)	$R_1 = 0.2003$, $wR_2 = 0.3300$		$R_1 = 0.1277$, $wR_2 = 0.3186$	
CCDC reference no.	281543		281544	

8.06 (br, 2H, Ar), 8.05 (d, *J* = 4 Hz, 2H, Por-β), 8.03 (d, *J* = 6 Hz, 2H, Py), 7.98 (t, *J* = 2 Hz, 2H, Ar), 1.56 (s, 18H, *t*-Bu), 1.55 (s, 18H, *t*-Bu), 1.49 (s, 18H, *t*-Bu), and 1.47 ppm (s, 18H, *t*-Bu); UV−vis (CHCl$_3$) λ_{max} = 426, 456, and 571 nm.

These aggregates have been examined by MALDI-TOF mass spectroscopy, which all showed peaks at the corresponding diporphyrin unit *m/z* = 1786.8 (calcd. for C$_{110}$H$_{106}$N$_{12}$O$_4$Zn$_2$ *m/z* = 1790.9) without no parent ion peaks of the aggregates.

X-ray Diffraction Analysis. Data collection for the compounds (**2**)$_3$ was carried out at −153 °C on a Bruker SMART APEX with graphite monochromated Mo$_{K}\alpha$ radiation (λ = 0.710 69 Å). Details of the crystallographic data are listed in Table 1. The structure was solved by direct methods (SHELXS-97)[17] and refined with full-matrix least-squares technique (SHLEXL-97).

The X-ray diffraction data set (*R*-**7**$_{out-out}$)$_5$ were collected at the BL44B2 beamline, SPring-8, Japan. Since the crystals of (*R*-**7**)$_5$ were very fragile and rapidly lost solvent in air, they were kept in mother liquor throughout handling and data collection. A Lindemann tube (0.5 mm) was used for sealing crystal, which was injected with high vacuum silicon grease (Dow corning) up to approximately 1 cm from the bottom of the tube and then filled with the mother liquor. Crystal was transferred into the tube, and let it sink until it touched the grease layer. To fix the crystal, it was then carefully pushed down with a thin glass capillary toward the grease layer so that it was partially buried in the layer. During data collection, neither crystal slippage nor damage of crystal was detected. The wavelength of the incident beam and sample− detector distance were set at 0.6000 Å and 140 mm, respectively. A total of 360 images with 1° oscillation were recorded using the ADSC Quantum 210 CCD detector system, which were processed and scaled using the program HKL2000 package[18] The structure was solved by the direct method with SHELXS-97. We could easily recognize the

pentagonal mainframes from the peaks that the program indicated. The mainframes of the *R*-**7**$_{out-out}$ structure were built based on the Zn sites with the program XFIT,[19] followed by refinement with SHELXL-97. Models for side chains were fitted to electron density map with coefficient of Fo-Fc. Some residual peaks in the solvent area were found in the electron density map, but none of them could be fitted as a solvent molecule. Because of the paucity of data, geometrical restraints were applied to chemically equivalent bonds and to make the phenyl and pyridyl groups planar. $wR_2 = 0.319$, $R_1 = 0.115$ [for 44571 refractions with $F^2 > 2\sigma(F^2)$], goodness of fit on $F^2 = 2.42$ on 4246 parameters. The absolute structure was determined to be *R* on the basis of anomalous dispersion (Flack parameter[20] 0.225(13).

The structure of (*R*-**7**$_{in-in}$)$_3$ was solved and refined with similar procedure to that of (*R*-**7**$_{out-out}$)$_5$. Eight toluene molecules and nine acetonitrile molecules could be assigned. $wR_2 = 0.438$, $R_1 = 0.188$ [for 12490 refractions with $F^2 > 2\sigma(F^2)$], goodness of fit on $F^2 = 1.97$ on 6950 parameters. The absolute structure was determined to be *R* on the basis of anomalous dispersion (Flack parameter[20] 0.04(4)).

CCDC-281543 ((**2**)$_3$), CCDC-281545 ((*R*-**7**$_{in-in}$)$_3$), and CCDC-281544 ((*R*-**7**$_{out-out}$)$_5$) contain the supplementary crystallographic data, which can be obtained free of charge from the Cambridge Crystallographic Data Centre via www.ccdc.cam.ac. uk/data_request.cif.

Supporting Information Available: GPC−HPLC chromatogram, chiral HPLC chromatogram, spectral data including CD, ^{1}H NMR in pyridine-*d*$_5$, X-ray analysis data and structures, and DFE calculated structures. This material is available free of charge via the Internet at http://pubs.acs.org.

JA0611137

(17) Sheldrick, G. M. SHELXS-97 and SHELXL-97, Program for the Solution and Refinement of Crystal Structures, University of Göttingen, Göttingen, Germany, 1997.
(18) Otwinowski, Z.; Minor, W. *Methods Enzymol.* **1997**, *276*, 307−326.
(19) McRee, D. E. In *Practical Protein Crystallography*; Academic Press: San Diego, CA, 1993.
(20) Flack, H. D. *Acta Crystallogr., Sect. A* **1983**, *39*, 876.